Open Access

Journal of Energy and Power Technology

LIDSEN Publishing Inc.

Original Research

A Large Eddy Simulation Study of Cyclones: The Effects of Interparticle Collisions on Erosion Prediction

Diego Alves de Moro Martins [1, *], João Rodrigo Andrade [2], Carlos Antonio Ribeiro Duarte [3], Ricardo de Vasconcelos Salvo [4], Francisco José de Souza [2, *]

1. Centro Federal de Educação Tecnológica de Minas Gerais, Av. Ministro Olavo Drummond, 25 Araxá, Brazil - ZIP: 38.180.510; E-Mail: diegomoro@cefetmg.br
2. Department of Mechanical Engineering, Federal University of Uberlândia, Fluid Mechanics Laboratory, Campus Santa Mônica, Uberlândia, Minas Gerais, Brazil - ZIP: 38400-902; E-Mails: joao.andrade@ufu.br; francisco.souza@ufu.br
3. Faculty of Engineering, Federal University of Catalão, Av. Dr. Lamartine Pinto de Avelar, 1120, Catalão, Goiás, Brazil; E-Mail: carlosduarte@ufcat.edu.br
4. Federal University of Technology - Paraná, Campus Londrina. Av. dos Pioneiros, 3131 Londrina - Parana, Brazil - ZIP: 86036-370; E-Mails: ricardosalvo@utfpr.edu.br

* **Correspondences:** Diego Alves de Moro Martins and Francisco José de Souza; E-Mails: diegomoro@cefetmg.br; francisco.souza@ufu.br

Academic Editor: Faik Hamad

Special Issue: Multi-phase Flow with and without Heat Transfer

Journal of Energy and Power Technology
2022, volume 4, issue 2
doi:10.21926/jept.2202017

Received: January 31, 2022
Accepted: April 26, 2022
Published: May 06, 2022

Abstract

Cyclone separators are widely used in fluid catalytic cracking (FCC) units due to their lack of moving parts and relatively low-pressure drop. However, cyclone separators are prone to erosion-related issues, which is a major drawback. In this paper, a large eddy simulation (LES) of the particle-gas flow in a cyclone separator is investigated using a four-way Euler-Lagrange approach to model inter-particle collisions and the exchange of momentum between particles and fluid. The effects of inter-particle and particle-wall collisions are characterized in terms of erosive wear. Additional effects involving the exchange of momentum between the fluid and

the particles are also discussed. The results show that considering the interparticle collisions between solid particles may be the key to predicting erosion.

Keywords
Cyclone erosion; four-way coupling; large eddy simulation; inter-particle collision; shielding effect

1. Introduction

In several engineering applications, a surface is struck by solid particles carried by a fluid, resulting in an undesired superficial wear of the equipment. This kind of abrasive wear is referred to as erosion, and frequently occurs in many industrial operations. In fluid catalytic cracking (FCC) units, catalyst particles are deliberately added to the process to accelerate chemical reactions. These particles are then separated and reused in a cyclical process. This separation is carried out by cyclone banks built into the reactor and regenerator of FCC units [1], and the mechanical wear caused by particles inside the cyclones is the main cause of unscheduled shutdowns in FCC units [2, 3]. Designing reliable tools to predict this behavior is the key to solving this issue and, thereby, both reducing cost and environmental complications due to potential spillage.

To date, only a few studies on erosion in cyclone separators have been published, very likely because of the complex nature of the phenomena [4]. Numerical and experimental studies were carried out by Danyluk et al. [5]. They carried out experiments using a Type 310 stainless steel cyclone from a medium Btu coal gasification process in a pilot plant. For the numerical analysis, the authors adopted a simplified two-dimensional flow pattern near the cyclone inner wall to compute particle trajectories, the results of which were used with Finnie's model [6]. Using this approach, the authors were able to achieve reasonable agreement between experimental and theoretical predictions for the lower half of the cyclone's inlet, but for the upper half of the inlet, they found substantial disagreement between results. They suggested that the disagreement was due to a deviation between the actual particle tracks and the flow pattern assumed in the model.

Zughbi et al. [7] investigated wear in the vortex finders of the dense media cyclones used in diamond mines using both numerical simulation and experimental measurements. They found that maximum wear always occurred in an area between 0 and 160 degrees of the cyclone feed inlet. Moreover, 52% of the points of maximum wear occurred at one point 90° from the inlet, implying that wear could be more evenly distributed around the vortex finder circumference by the use of double-entry cyclones. For the numerical simulations, axisymmetry was assumed, which allowed the use of a two-dimensional model, while the flow was also assumed to be steady. Using commercial PHOENICS® software, they found that numerical estimations of vortex finder wear showed a similar trend to the experimental results.

Dobrowolski et al. [4] numerically studied erosion wear in cyclone separators. For this, they used the Fluent® software package and the particle-in-cell (PIC) method, assuming the continuous phase to be isothermal and steady and adopting a $\kappa - \epsilon$ turbulence model. For prediction of the erosion process, they chose the Bitter model, in which the erosion mechanism is characterized by shearing

and deformation. They concluded from the results of the simulation that the upper cylindrical part of the cyclone separator was subject to erosion.

Blaser et al. [3] performed computational simulations of FCC reactor cyclones at the Catlettsburg refinery (Kentucky, USA) to mitigate severe erosion. They modeled the erosion using the Barracuda Virtual Reactor™ software package and the Eulerian-Lagrangian transient approach as an alternative to the Particle-In-Cell method. They stated that, although the results of the erosion model are qualitative, they were able to identify the regions with the highest likelihood of erosion as being the short side of the crossover, the top side of the crossover, and the inlet sweep area of the cyclone main body.

Kan and Liu [8] analyzed the erosion process in electro-cyclone separators by considering Stokes, centrifugal, and electrostatic forces. They were able to conclude that the erosion wear on the cone of an electro-cyclone is similar but more severe than the erosion wear observed in conventional cyclones and was directly related to the voltage applied. They were also able to conclude that particles bigger than 40 μm accelerated the erosion rate.

Arabnejad et al. [9] performed experiments and numerical simulations to study erosion in a laboratory-scale gas-liquid cylindrical cyclone separator under both gas-sand and gas-liquid-sand flow conditions. They used an ultrasonic system to monitor the erosion rates in the test facility and commercial software for the CFD simulations. They opted to use the Shear Stress Transport (SST) $\kappa - \omega$ turbulence model and a one-way coupling with the dispersed phase in the simulations. Based on the results of the experiments and CFD simulations, they proposed a mechanistic model for the maximum thickness loss computation.

Parvaz et al. [10] used the Fluent® software package to simulate modified cyclone separators and evaluated the differences in performance and erosion rates obtained through such modifications. They adopted the Eulerian-Lagrangian approach with one and two-way coupling for erosion prediction. Eulerian phase turbulence was modeled using the RSM turbulence model, while the discrete random walk (DRW) method was used to evaluate the velocity fluctuations of the gas in the Lagrangian computations. They concluded that the conventional (unmodified) cyclone experienced the highest erosion rate.

Reppenhagen and Werther [11] investigated, theoretically and experimentally, the mechanism of catalyst attrition in cyclones for various catalysts. While, numerical simulations were made by Utikar et al. [12] to predict erosion in cyclone separators, using the Eulerian-Lagrangian approach with two-way coupling.

It is interesting to note that in most of the above-mentioned works, although the exact position changes from study to study, the highest erosion rates are said to occur close to the tangential entrance and the cone bottom. The relationship between velocity and erosion is another common factor, as it is expected that the velocity of the fluid and particles plays a crucial role in erosion. The authors of reference [9] even suggest that setting a uniform injection velocity for particles may lead to excessive erosion. However, while it is known that such interparticle collisions tend to reduce erosion rates in bends [13-16], to the best of the authors' knowledge, no systematic study of these effects has been carried out in cyclones, something that can only be accomplished by numerical simulations. The main aim of this current work is to investigate the effects of interparticle collisions on cyclone erosion.

The proper utilization of Computational Fluid Dynamics (CFD) enables accurate simulation of the flow of fluids, such as oil or gas [17]. It also allows the accurate prediction of particle motion within

fluid flow by tracking the particles and their interactions with the walls and each other. Once the particle paths are known, together with empirical correlations relating to the properties of the particles and the eroded material, erosion can easily be estimated from the impact velocity and impact angle. An important consideration with CFD is how to deal with turbulence, which results in highly complex interactions between different wavenumbers [18-20]. Direct Numerical Simulations (DNS) are the most accurate approach; however, the computational cost incurred is too high for most industrial problems. Reynolds-Averaged Navier-Stokes simulations (RANS) are a viable alternative approach and applicable to complex geometries at high Reynolds numbers. However, the embedded simplifications come at the expense of accuracy. For example, particles are carried by the instantaneous flow field, which is not directly calculated in RANS. A particle dispersion model is then necessary, requiring additional modeling, which in turn affects the final accuracy of the results. It should be pointed out that all the above-mentioned works that used CFD performed RANS only. In the current study, we have opted instead to use the Large Eddy Simulation (LES) approach, as this represents a compromise solution between the RANS modeling and DNS. For particle modeling, we have adopted the Lagrangian framework, as interactions between both phases are straightforwardly accounted for using this approach. The coupling between the gas and solid phases was also investigated.

The work of Karri et al. [21] was used as an experimental reference for the numerical simulations. However, as their experiments were accomplished in a cyclone with a drywall coating, different from the materials employed in the present models, the comparison between the numerical and experimental results was performed in a qualitative way only.

Our findings show that erosion rates are higher when interparticle collisions are included in the simulations, which may be because such collisions cause more particle dispersion and consequently affect new areas other than those originally impacted. We also conclude that the use of simulations with four-way coupling is important when tacking cyclone erosion.

2. Mathematical Models

The Euler-Lagrange approach was used in this study, while the continuous phase was solved using Large Eddy Simulation (LES) modeling, and particle motion was based on Newton's second law. The modeling of the two phases and the erosion are briefly described below.

2.1 Gas-Phase Model

Filtered continuity and the Navier-Stokes equation (Eqs. (1-2)) with a Smagorinsky turbulence model [22] were adopted for modeling the gas phase. This sub-grid scale model was chosen due to its good accuracy when solving turbulent rotational flows [23]. Full details of the fluid phase modeling and its equations can be found in the authors' previous works [23, 24].

$$\frac{\partial(\rho\bar{u_\iota})}{x_i} = 0 \tag{1}$$

$$\frac{\partial(\rho\bar{u_\iota})}{\partial t} + \frac{\partial\left(\rho\bar{u_\iota}\bar{u_j}\right)}{\partial x_j} = -\frac{\partial\bar{p}}{\partial x_i} + \frac{\partial}{\partial x_j}\left[(\mu+\mu_t)\left(\frac{\partial\bar{u_\iota}}{\partial x_j} + \frac{\partial\bar{u_j}}{\partial x_i}\right)\right] + S_{\pi_p} \tag{2}$$

where the overbar is a filtered quantity, S_{π_p} is the source term due to interaction with the dispersed phase, ρ and μ are the fluid density and viscosity, respectively, and μ_t is the eddy viscosity given by Eq (3).

$$\mu_t = (\rho Cs\Delta^2)\overline{S} \tag{3}$$

where Δ is the spatial filter length, $\overline{S}$ is the filtered shear strain rate, and Cs is given by the Van Driest damping function.

2.2 Particle Motion Model

The dispersed phase was treated in a Lagrangian framework with the trajectory, linear momentum, and angular momentum conservation equations (Eqs. (4-6)) being solved at time steps, allowing each particle to be tracked through the domain.

$$\frac{\mathrm{d}x_{pi}}{\mathrm{d}t} = u_{pi} \tag{4}$$

$$m_p \frac{\mathrm{d}u_{pi}}{\mathrm{d}t} = m_p \frac{3\rho C_D}{4\rho_p d_p}\left(\bar{u_i} - u_{pi}\right) + F_{si} + F_{ri} + \left(1 - \frac{\rho}{\rho_p}\right) m_p g_i \tag{5}$$

$$I_p \frac{\mathrm{d}\omega_{pi}}{\mathrm{d}t} = T_i \tag{6}$$

where $\bar{u_i}$ is the filtered fluid velocity interpolated to the particle position, u_{pi} and ω_{pi} are the linear and angular particle velocity, respectively, d_p and ρ_p are the particle diameter and particle density, respectively, C_D is the drag coefficient, F_{si} is the shear-induced lift force, F_{ri} is the rotation-induced lift, T_i is the particle torque, and I_p is the particle moment of inertia.

The source term presented in Eq. (2) is responsible for momentum transfer from particles to fluid. This term is detailed in Eq. (7).

$$S_{\pi_p} = \frac{-1}{V_{cv}} \sum_K m_k N_k \times \frac{1}{\Delta_t} \sum_n \left[\left[\left(u_{pi}\right)_k^{(n+1)} - \left(u_{pi}\right)_k^n \right] - g_i \left(1 - \frac{\rho}{\rho_p}\right) \Delta t_L \right] \tag{7}$$

Where k is related to the number of computational particles that passed through the cell, m_k is the mass of each particle that passes through the cell, N_k is the number of real particles that a computational particle represents, n is the number of sub-time-steps used for computational particle time advancement, and Δt_L is the Lagrangian time-step. Inter-particle collisions are modeled using a stochastic, hard-sphere model [25]. A full description of the particle forces used in the present work is given in references [16] and [26].

When a particle collides with a wall, its new linear and angular velocities after rebound are calculated according to the following conservation equations described by [27]:

Non-sliding collision:

$$\vec{u}_p^{+} = \vec{u}_p^{-} - \left(1 + e_{par}\right) \frac{2}{7} \vec{u}_{pr}^{-} - (1 + e)\left(\vec{u}_p^{-} \cdot \vec{n}\right) \vec{n} \tag{8}$$

$$\vec{\omega}_p^{+} = \vec{\omega}_p^{-} - \frac{10}{7}\frac{1 + e_{par}}{d_p}\,\vec{n} \times \vec{u}_{pr}^{-} \tag{9}$$

Sliding collision:

$$\vec{u}_p^{+} = \vec{u}_p^{-} - (1 + e)\left(\vec{u}_p^{-} \cdot \vec{n}\right)\left[\mu_d \frac{\vec{u}_p^{-}}{\left|\vec{u}_p^{-}\right|} + \vec{n}\right] \tag{10}$$

$$\vec{\omega}_p^{+} = \vec{\omega}_p^{-} - \frac{5}{d_p}(1 + e)\left(\vec{u}_p^{-}.\vec{n}\right)\frac{\mu_d}{\left|\vec{u}_p^{-}\right|}\vec{n} \times \vec{u}_{pr}^{-} \tag{11}$$

where the superscripts $-$ and $+$ denote values before and after the collision, respectively, e_{par} is the parallel restitution coefficient, e is the normal restitution coefficient, μ_d is the dynamic friction coefficient, $\vec{n}$ is the normal unit vector pointing outwards of the element face being impacted, and $\vec{u}_{pr}$ is the relative velocity at the contact point:

$$\vec{u}_{pr} = \vec{u}_p - \left(\vec{u}_p \cdot \vec{n}\right)\vec{n} + \frac{d_p}{2}\,\omega_p \times \vec{n} \tag{12}$$

2.3 Erosion Model

The erosion ratio and its simulation parameters are given by the correlations contained in reference [28]. The erosion model has been extensively validated by the authors of the current work in previous publications [13, 14, 29, 30]. The empirical restitution correlation proposed by [31] was added to the simulations in this current work. The erosion model equations, Eqs. (13-18), are:

$$E(\alpha) = g(\alpha)E_{90} \tag{13}$$

$$g(\alpha) = \left(sen(\alpha)\right)^{n_1}\left[1 + H_v\left(1 - sen(\alpha)\right)\right]^{n_2} \tag{14}$$

$$E_{90} = 81{,}714(H_v)^{-0{,}79}\left(\frac{V_p}{V_p{}^*}\right)^{k_2}\left(\frac{D_p}{D_p{}^*}\right)^{k_3} \tag{15}$$

where $E(\alpha)$ and E_{90} denote a unit of eroded material per mass of particles (mm^3/kg), $g(\alpha)$ is the impact angle dependence function, H_v is the initial eroded material Vickers hardness number (GPa), and V_p and D_p are the impact velocity and particle diameter, respectively. The constants n_1, n_2, k_2 and k_3 were set for an SiO_2- aluminum pair [28].

The conversion of $E(\alpha)$ into the erosion ratio E_t is achieved using the following conversion factor, (16):

$$E_r = 1{,}0 * 10^{-9}\rho_w E(\alpha) \tag{16}$$

$$E_t = \frac{1}{A_f}\sum_{m_f}\dot{m}_\pi E_r \tag{17}$$

$$RP = \frac{E_t}{\dot{m}\rho_w} \tag{18}$$

where ρ_w is the wall density, A_f is the area of the face collided, $\dot{m}_\pi$ is the particle mass flow rate represented by each computational particle that collides with the face, RP is the penetration ratio, and $\dot{m}$ is the particle mass flow rate.

Friction is another important effect to be accounted for in particle-to-wall interactions. Depending on the static and dynamic coefficients, particles can lose energy and momentum through fiction, directly affecting their movement and, consequently, the erosion process. In the present study, both the static and dynamic coefficients of friction were assumed to be 0.25 and the wall to be perfectly smooth.

The influence of the type of phase coupling assumed - one-way, two-way, or four-way was investigated. In one-way coupling, it is assumed that the fluid forces influence particle behavior, but the fluid itself is not influenced by the particles., while, in two-way coupling, there is an exchange of momentum between the phases; and, in four-way coupling, there is an exchange of momentum between the phases and between the particles. More details on these different models can be found in [30, 32].

3. Numerical Models

The numerical solution of the transport equations is accomplished by the unstructured grid code UNSCYFL3D, which has been extensively validated for turbulent, single-phase, and particle flow simulations [13, 15, 33-37]. This in-house tool is based on the finite-volume approach in unstructured three-dimensional grids. In this work, only the unsteady-state solution for the fluid was sought. The central differencing scheme was used for the advective and diffusive terms of the momentum equations.

4. Test Case Description

The cyclone separator employed in the simulations was the same as that used by Utikar et al. [12] in their experiments. Figure 1 shows a schematic diagram of the experimental cyclone and its dimensions.

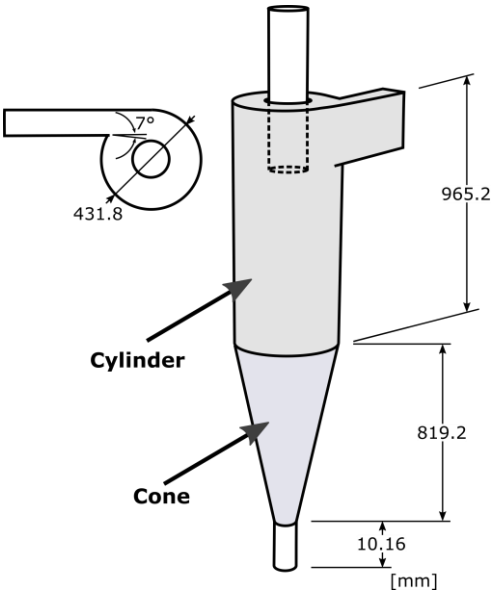

Figure 1 Schematic diagram of the experimental cyclone (reference [12]).

The Utikar et al. experiments were carried out in a cyclone with multiple coatings of drywall joint compound added to its inner walls, with equilibrium FCC catalyst particles with a median diameter of 75 µm. The experimental conditions were set to be similar to those of a second-stage cyclone present in real FCC units. The fluid was air, and the boundary conditions were given as: inlet velocity 19.8 m/s, Reynolds number $Re = 5.4 \times 10^5$, particle mass flow rate $\dot{m}_p = 4.05 \times 10^{-3}[kg/s]$, and gas mass flow rate of $\dot{m}_g = 4.446 \times 10^{-1}[kg/s]$ resulting in a mass loading of $9.12 \times 10^{-3}\ kg_p/kg_g$.

The amount of erosion in the cyclone was characterized as the weight loss of the drywall compound over time, and the experimental results showed that the erosion took place primarily in the cone of the secondary cyclone.

For our numerical simulations, we used the same parameters. However, some simplifications were made to successfully realize the simulations. The particles were considered spherical, whereas the particles in the experimental study had an angular shape. No correlations for friction, restitution, and erosion could be found in the literature for a catalyst-drywall pair. So correlations for a sand-aluminum pair were used. The particle residence time was set to 0.5 s, and in all simulations, nine residence times were simulated to provide converged statistics. The time step used for both the fluid and the particles was 5×10^{-5} s.

For the particle phase simulation, five parcels were injected at each time step. For the final step, about 300,000 computational particles were simulated to obtain statistically-converged particle velocities and concentration fields. To determine the number of parcels for statistical convergence, preliminary simulations were run with monitoring of the maximum erosion rates. Although this exercise showed that fewer than 300,000 parcels would suffice, it was decided to inject many more to produce smooth erosion contours and avoid the unphysical deformations reported by Solnordal and Wong [38]. Table 1 gives the simulation parameters.

Table 1 Simulation parameters.

Cyclone material	Aluminum (6061-T6)
Cyclone density	2,700 kg/m^3
Vickers hardness	1.049 GPa
Particle type	SiO_2
Particle density	1.490 kg/m^3

ANSYS ICEM-CFD software and an O-grid meshing technique were used to generate unstructured three-dimensional hexahedra near the wall regions, where high-velocity gradients and boundary layer are present (Figure 2). The total number of elements generated for the entire domain was approximately 1,800.000, which yielded mesh-independent results. This number was arrived at by examining the pressure drop through the system and the maximum erosion rate for three successively finer grids. The GCI (Grid Convergence Index) proposed by Roache [39] was used to determine the necessary resolution.

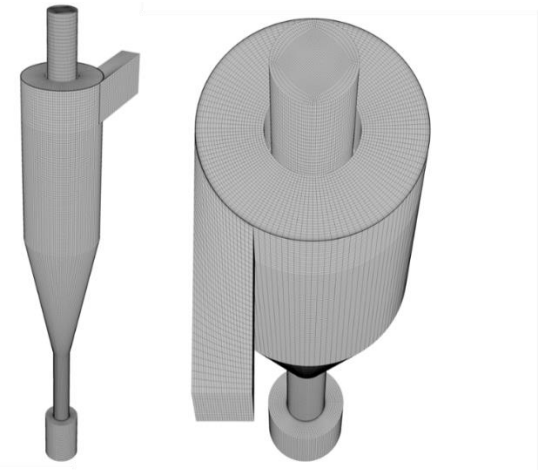

Figure 2 Computational mesh (ANSYS ICEM-CFD software).

5. Results and Discussion

In our numerical simulations, we focused on the analysis of the parameters that are most important for understanding the erosion phenomenon in this equipment - $i.e.$, particle distribution over the domain, wall impact frequency, particle velocity, impact angle, and penetration ratio.

Figure 3 shows the particle distribution at the last time step computed for each of the three phase coupling methods. As can be seen, there were no observable differences between the models. This may be because of the low mass loading inside the cyclone - the concentration is not visibly altered by the interparticle collisions. The particle concentration is qualitatively higher in the cone bottom region, which is due to the high angular velocity and low axial velocity. This was as expected due to the progressive reduction in the cone radius. Interestingly, there is also evidence of particles concentrating at the top of the cyclone cylinder, particularly for the four-way method.

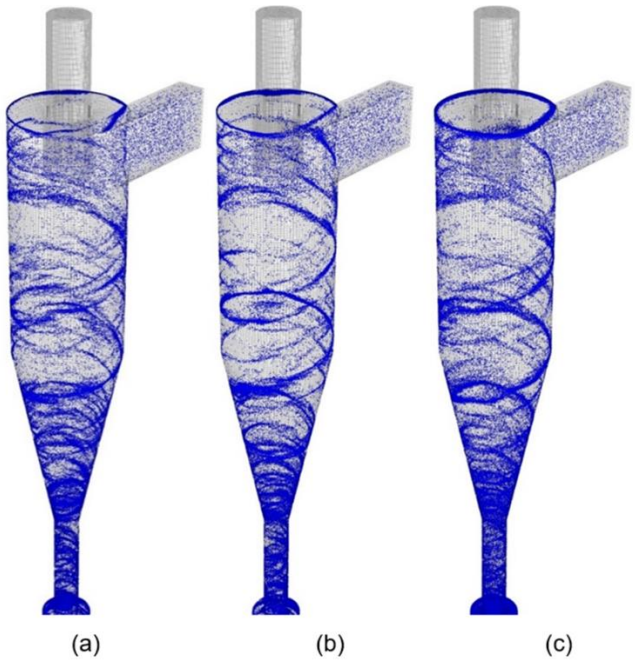

Figure 3 Simulated particle distribution for the one-way (a), two-way (b), and four-way (c) coupling methods.

To analyze the particle distribution inside the domain, the contour of the particle concentration in an XY plane highlighting the interparticle collision effect was studied (Figure 4). As it can be seen, interparticle collisions, modeled by the four-way coupling method, cause a layer of increased concentration in the vicinity of the wall. This can be attributed to the "cushioning effect" of particles near the wall preventing incoming particles from interacting with the wall. These tests also showed a high particle accumulation at the upper corner of the cyclone cylinder, which may be associated with a combination of lift force and interparticle momentum exchange as is intensified for the four-way modeling.

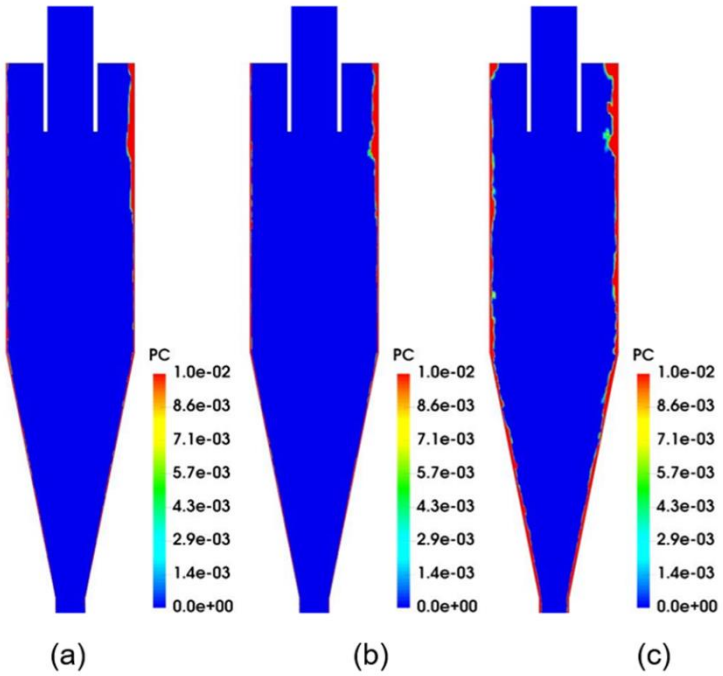

Figure 4 The contour of the particle concentration in the *XY* plane for the one-way (a), two-way (b), and four-way (c) coupling methods.

Figure 5 shows the impact frequency contour for each phase coupling method. Unsurprisingly, there was a significant positive correlation between impact frequency and particle concentration. At the same time, the local values for the impact frequency were lower and more scattered with the four-way coupling method, which could also be attributed to the cushioning effect.

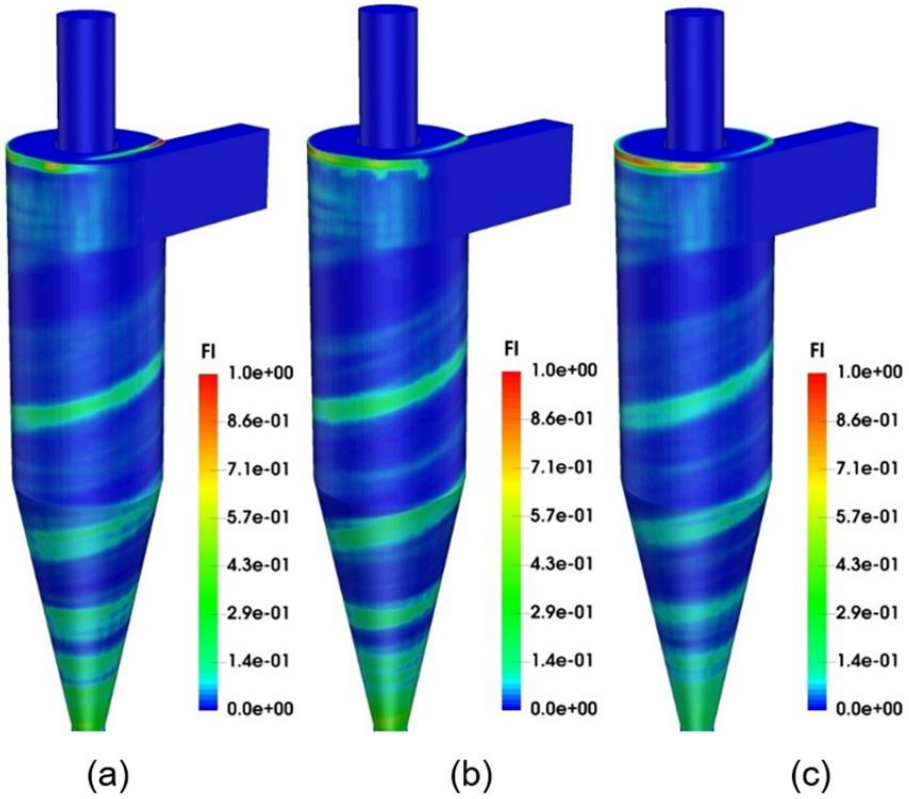

Figure 5 The contour of the impact frequency for the one-way (a), two-way (b), and four-way (c) coupling methods.

Figure 6 shows the particle impact frequency profile from bottom to top extracted along the cylinder wall on the opposite side to the cyclone inlet obtained from the time-averaged values of the simulations. As can be seen, the impact frequency is smaller with four-way coupling over the entire domain, with a single exception - there is a peak in the curve on the upper part of the cyclone cylinder, $d \approx 0.95$. Interestingly, thanks to the use of the Large Eddy Simulation turbulence approach, it was possible to observe high-frequency variations in these results (Figure 6), indicating that the particles are clustered in oscillatory regions, with peaks and troughs. This effect is dampened with the four-way model and possibly occurs through momentum transfer between the particles.

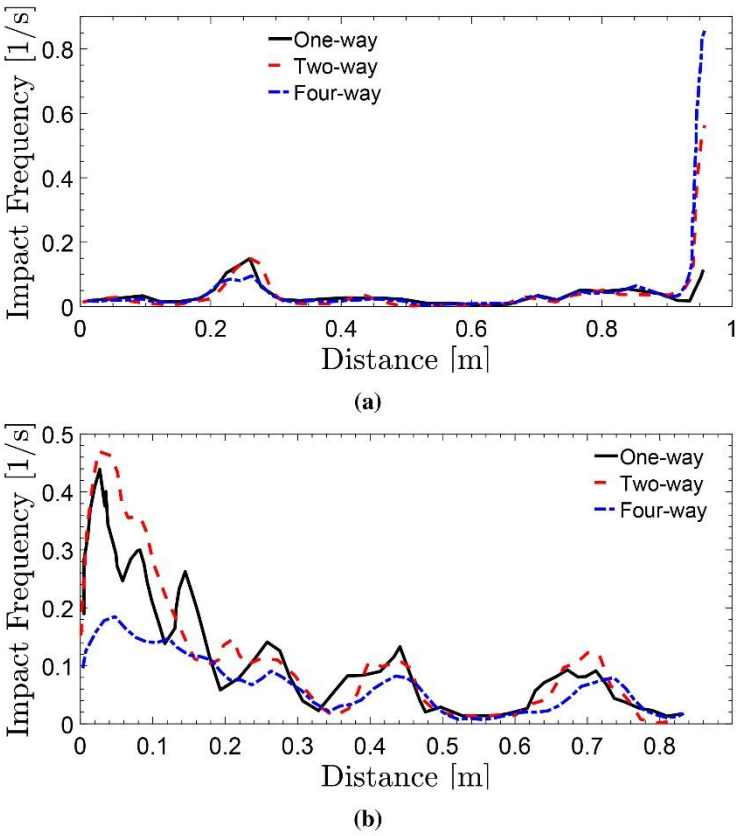

Figure 6 Impact frequency profile from top to bottom along the cylinder wall (a) and cone (b).

Along with impact angle and impact velocity, material properties are the most important factors in erosion. Thus, it is important to analyze the effect of the different coupling methods on these variables. Figure 7 shows the particle impact angle contour for each phase coupling method. As expected, the regions with the higher impact angle are opposite the cyclone inlet, where the particles enter with high velocity, while the impact angle decreases as particles get closer to the outlets. Differences between the models can be observed that are more intense in the cone locations, which indicates that, in this region, momentum exchange between particles has a significant impact on the impact angle.

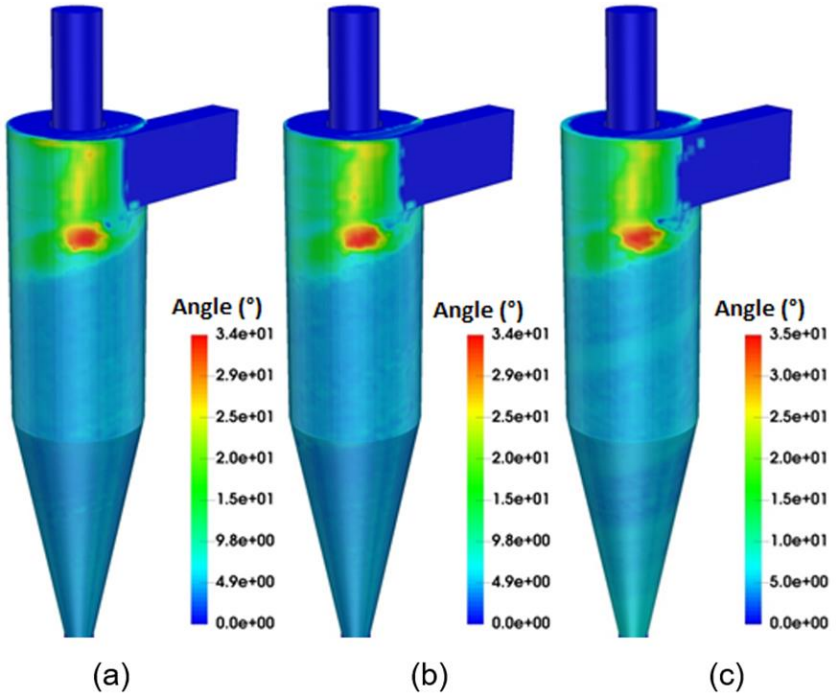

Figure 7 Particle impact angle contours for the one-way (a), two-way (b), and four-way (c) coupling methods.

To better understand the differences between each model in the cyclone cone, the impact angle profile along this region was examined (Figure 8). This showed that the impact angle increases over the whole domain when momentum exchange between particles is considered. This is a significant result as the impact angle plays a very important role in erosion calculations.

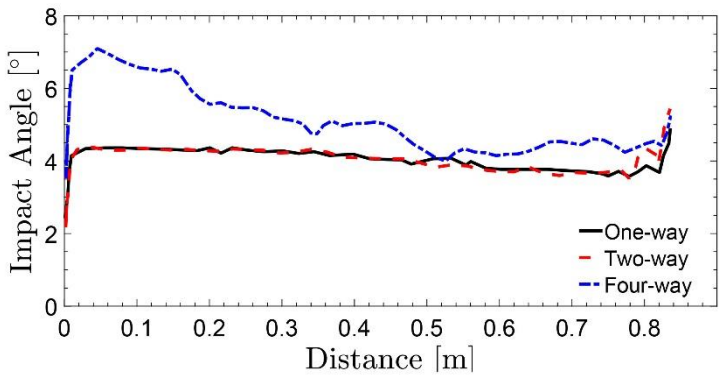

Figure 8 The impact angle profile along the cyclone cone, from bottom to top.

Figure 9 shows the particle impact velocity contour for each phase coupling method. No great differences between the models can be observed. This indicates that momentum exchange between particles has no significant correlation with impact velocity. As expected, and like the impact angle, peak impact velocities are found opposite the cyclone inlet, while the particle impact velocity decreases as the particles approach the outlets.

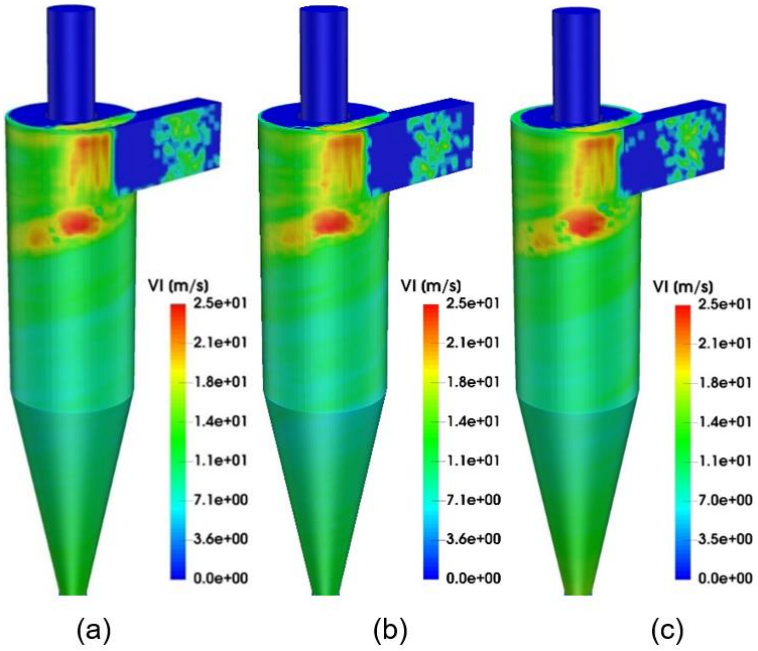

Figure 9 Particle impact velocity contours for the one-way (a), two-way (b), and four-way (c) coupling methods.

Figure 10 shows the penetration ratio contour for each phase coupling method. As with the experiments performed by Utikar et al. [12], the cone bottom is the most eroded region. This is due to the high particle concentration and high impact frequency in this region, as shown in the previous figures. Erosion near the cyclone inlet was also observed in experiments, which is a consequence of a higher impact velocity combined with a moderate impact angle.

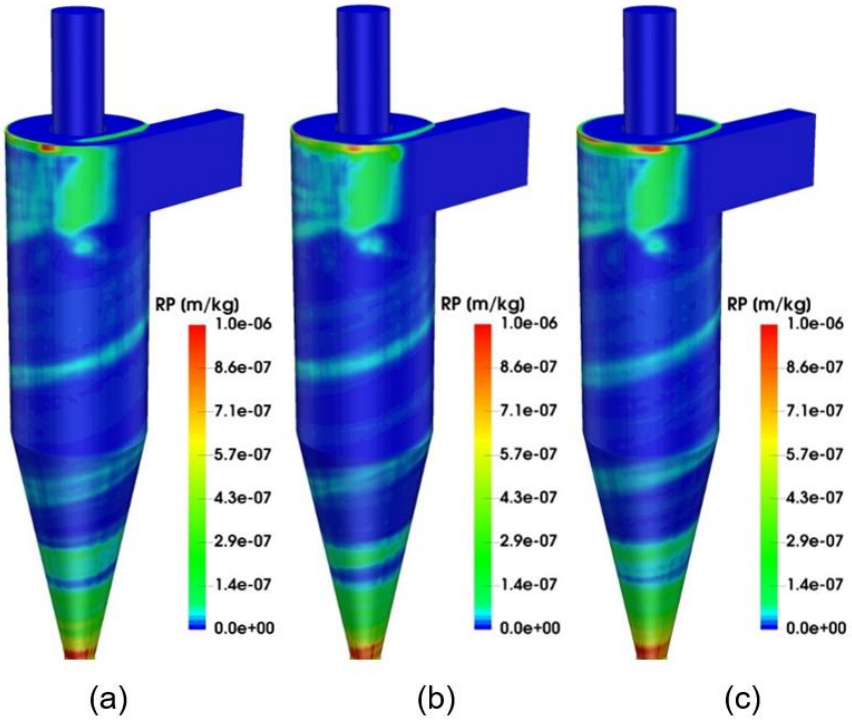

Figure 10 Penetration ratio contours for the one-way (a), two-way (b), and four-way (c) coupling methods.

As Figure 11 shows, the penetration ratio changes according to the modeled effects, particularly when the four-way coupling method is applied, which is due to the "cushioning effect" that takes place at the bottom of the cone. In this location, the penetration ratio is small compared to that of the one-way and two-way coupling methods. This effect can be related to the low impact frequency shown in Figure 6 for this coupling method.

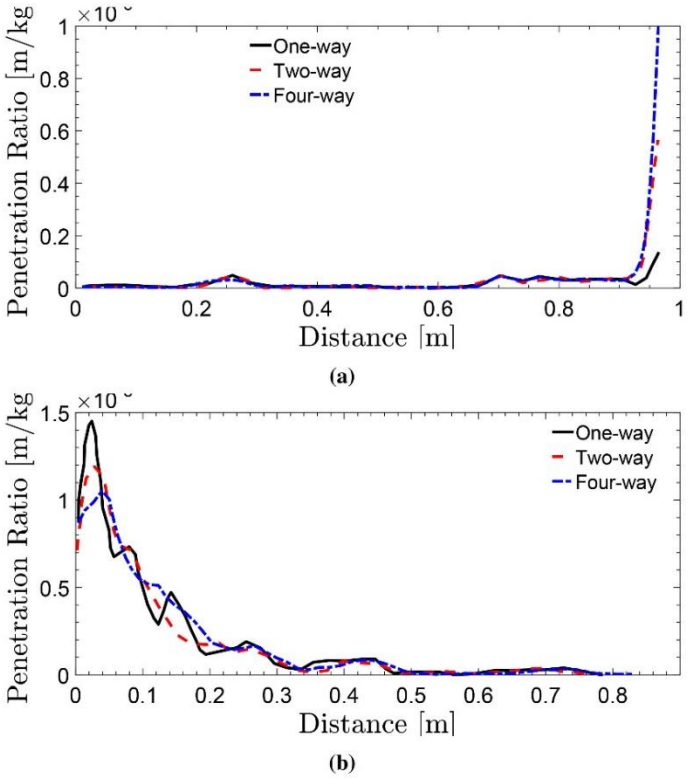

Figure 11 The penetration ratio profile along the cylinder (a), and cone (b), from bottom to top.

A high particle concentration is found in the cylinder's upper region (Figure 4), and consequently, the penetration ratio was greatest in this region. The penetration ratio was also widely distributed along the wall with the four-way method due to interparticle collisions causing a scattering of the particles along the wall. This scattering of particles and the relatively high impact velocity and angle cause an increase in the penetration ratio with the four-way coupling method. This effect can be observed numerically in the results presented in Table 2, which show the erosion rate obtained in the cyclone for each phase coupling and area of the cyclone.

Table 2 Erosion rates [g/h] generated from the simulations.

Coupling methods	Cylinder	Cone	Total
One-way	0.2559	0.7039	0.9629
Two-way	0.2686	0.6750	0.9436
Four-way	0.3007	0.8234	1.1241
Experimental	105	680	785

As it can be seen from Table 2, the erosion rates obtained experimentally are much higher than those obtained by simulation. This is due to the material properties employed in the simulations. Specifically, aluminum has a higher abrasion resistance than drywall. However, the trends in erosion rates are similar, which shows the predictive ability of the current models. To perform a quantitative comparison, empirical correlations for the same pair of materials used in the experiments must be developed.

6. Conclusions

This paper investigated the use of numerical simulations to predict erosion in cyclone separators. The numerical model included both gas-solid interactions and interparticle collisions using a four-way coupling model with the Eulerian-Lagrangian approach. While turbulence was modeled using the Large Eddy Simulation procedure. The simulation results were compared to the experiments made by Utikar et al. [12] under similar conditions. This comparison showed that there was no significant difference in the trend in erosion between the numerical and the experimental data. However, due to the model simplifications - the computational model is adapted to spherical sand particles and aluminum walls, while the experiments were carried out with angular catalyst particles and drywall wall joint compound - differences were found in the magnitude of the erosion.

A comparison between different phase coupling approaches (one-way, two-way, and four-way) was also conducted. No significant difference between one-way and two-way coupling methods was observed, due probably to the low mass loading employed in the experiment. To verify the influence of momentum exchange between phases, further tests with higher mass loadings are required.

The penetration ratio obtained using the four-way coupling method is slightly higher than that obtained using the other methods, which can be attributed to interparticle collisions promoting higher dispersion between the particles. The higher spread increases the size of the region where the particles impact the wall, resulting in an enlarged wear area. The particle cushioning effect near the wall was also captured in the simulations. This finding confirms the importance of using the four-way approach when modeling complex equipment like a cyclone. And we conclude that the use of four-way coupling is necessary for the acquisition of reliable data through computer simulations in this domain.

Acknowledgments

The authors would like to acknowledge the financial technical support from the Petróleo Brasileiro S.A. (Petrobras) and the Brazilian funding agencies Coordenadoria de Aperfeiçoamento de Pessoal de Nível Superior (CAPES), Conselho Nacional de Desenvolvimento Científico e Tecnológico (CNPq) and the Fundação de Amparo à Pesquisa do Estado de Minas Gerais (FAPEMIG).

Author Contributions

Diego Alves de Moro Martins: execution, code writingqdebugging; João Rodrigo Andrade: editing/analysis of results; Carlos Antonio Ribeiro Duarte: editing/analysis of results; Ricardo de Vasconcelos Salvo: editing/analysis of results; Francisco José de Souza: funding acquistion, editing.

Competing Interests

The author has declared that no competing interests exist.

References

1. Sadeghbeigi R. Fluid catalytic cracking handbook: An expert guide to the practical operation, design, and optimization of FCC units. Butterworth Heinemann; 2020.
2. Chen YM. Evolution of FCC - past present and future and the challenges of operating a high temperature CFB system [Internet]. 10th International Conference on Circulating Fluidized Beds and Fluidization Technology; 2013. Available from: https://dc.engconfintl.org/cfb10/72.
3. Blaser P, Thibault s, Sexton J. Use of computational modeling for fcc reactor cyclone erosion reduction at the marathonpetroleum catlettsburg refinery [Internet]. The 14th International Conference on Fluidization - From Fundamentals to Products - JAMKuipers, ECI Symposium Series; 2013. Available from: http://dc.engconfintl.org/fuidization xiv/92.
4. Dobrowolski B, Skulska M, Wydrych J. Numerical modeling of erosion wear of components of cyclone separators. Archiwum Energetyki. 2008; 38: 63-70.
5. Danyluk S, Shack WJ, Park JY, Mamoun MM. The erosion of a type 310 stainless steel cyclone from a coal gasification pilot plant. Wear. 1980; 63: 95-104.
6. Finnie I. Erosion of surfaces by solid particles Oberflächenerosion durch feste teilchen. Wear. 1960; 3: 87-103.
7. Zughbi HD, Schawarz MP, Turner WJ, Hutton W. Numerical and experimental investigations of wear in heavy medium cyclones. Miner Eng. 1991; 4: 245-262.
8. Kan LF, Liu WJ. Analysis of the inner surface erosion wear at cone parts of electro-cyclone separators. Am Int J Contemp Res. 2015; 5: 59-66.
9. Arabnejad H, Sajeev S, Guimmarra A, Vieira R, Shirazi SA. Experimental study and modeling of sand erosion in the gas-liquid cylindrical cyclone GLCC separators [Internet]. Society of Petroleum Engineers; 2016. Available from: https://onepetro.org/SPEATCE/proceeding abstract/16ATCE/1-16ATCE/D011S001R002/185121.
10. Parvaz F, Hosseini SH, Elsayed K, Ahmadi G. Numerical investigation of effects of inner cone on flow field, performanceand erosion rate of cyclone separators. Sep Purif Technol. 2018; 201: 223-237.
11. Reppenhagen J, Werther J. Catalyst attrition in cyclones. Powder Technol. 1999; 113: 55-69.
12. Utikar R, Darmawan N, Tade M, Li Q, Evans G, Glenny M, et al. Hydrodynamic simulation of cyclone separators. In: Computational Fluid Dynamics. BoD - Books on Demand; 2010. pp. 241-266.
13. Duarte CAR, De Souza FJ, dos Santos VF. Numerical investigation of mass loading effects on elbow erosion. PowderTechnol. 2015; 283: 593-606.
14. dos Santos VF, de Souza FJ, Duarte CAR. Reducing bend erosion with a twisted tape insert. Powder Technol. 2016; 301: 889-910.
15. Duarte CAR, De Souza FJ, de Vasconcelos Salvo R, dos Santos VF. The role of inter-particle collisions on elbow erosion. Int J Multiph Flow. 2016; 89: 1-22.
16. Duarte CAR, de Souza FJ. Innovative pipe wall design to mitigate elbow erosion: A CFD analysis. Wear. 2017; 381:176-190.

17. Martins RS, Andrade JR, Ramos R. On the effect of the mounting angle on single- path transit-time ultrasonic flowmeasurement of flare gas: A numerical analysis. J Braz Soc Mech Sci. 2020; 42: 13.
18. Jacob B, Ribeiro Duarte LE, Andrade JR, Ribeiro Duarte CA. Effects of random disturbances on the stability of a temporallyevolving incompressible plane wake. Mech Res Commun. 2020; 102: 103475.
19. Andrade JR, Martins RS, Mompean G, Thais L, Gatski TB. Analyzing the spectral energy cascade in turbulent channelflow. Phys Fluids. 2018; 30: 065110.
20. Andrade JR, Martins RS, Thompson RL, Mompean G, Da Silveira Neto A. Analysis of uncertainties and convergence ofthe statistical quantities in turbulent wall-bounded flows by means of a physically based criterion. Phys Fluids. 2018; 30: 0451006.
21. Karri RSB, Cocco R, Knowlton T. Erosion in second stage cyclones: Effects of cyclone length and outlet gas velocity [Internet]. 10th International Conference on Circulating Fluidized Beds and Fluidization Technology; 2011. Available from: https://dc.engconfintl.org/cfb10/40.
22. Smagorinsky J. General circulation experiments with the primitive equations. Mon Weather Rev. 1963; 91: 99-164.
23. De Souza JF, de Vasconcelos Salvo R, de Moro Martins DA. Large eddy simulation of the gas-particle flow in cyclone separators. Sep Purif Technol. 2012; 94: 61-70.
24. De Moro Martins DA, de Souza FJ, de Vasconcelos Salvo R. Formation of vortex breakdown in conical-cylindrical cavities. Int J Heat Fluid Flow. 2014; 48: 52-68
25. Sommerfeld M. Validation of a stochastic lagrangian modelling approach for interparticle collisions in homogeneousisotropic turbulence. Int J Multiphase Flow. 2001; 27: 1829-1858.
26. De Souza FJ, Silva AL, Utzig J. Four-way coupled simulations of the gas- particle flow in a diffuser. Powder Technol. 2014; 253: 496-508.
27. Breuer M, Alleto M, Langfeldt F. Sandgrain roughness model for rough walls within eulerian-lagrangian predictions ofturbulent flows. Int J Multiphase Flow. 2012; 43: 157-175.
28. Oka YI, Okamura K, Yoshida T. Practical estimation of erosion damage caused by solid particle impact. Wear. 2005; 259: 95-101.
29. Duarte CAR, de Souza FJ, Venturi DN, Sommerfeld M. A numerical assessment of two geometries for reducing elbowerosion. Particuology. 2020; 49: 117- 133.
30. Duarte CAR, de Souza FJ, de Vasconcelos Salvo R, dos Santos VF. The role of inter-particle collisions on elbow erosion. Int J Multiphase Flow. 2017; 89: 1-22.
31. Grant G, Tabakoff W. Erosion prediction in turbomachinery resulting from environmental solid particles. J Aircr. 1975; 12: 471-478.
32. Crowe CT, Michaeides E, Schwarzkopf JD. Multiphase Flow Handbook. 2nd ed. CRC Press; 2005.
33. Duarte CAR, De Souza FJ, Dos Santos VF. Mitigating elbow erosion with a vortex chamber. Powder Technol. 2016; 288: 6-25.
34. De Souza FJ, de Vasconcelos Salvo R, de Moro Martins DA. Large Eddy Simulation of the gas-particle flow in cyclone separators. Sep Purif Technol. 2012; 94: 61-70.
35. De Souza FJ, Silva AL, Utzig J. Four-way coupled simulations of the gas-particle flow in a difuser. Powder Technol. 2014; 253: 496-508.
36. Duarte CAR, Duarte LER, de Lima BS, de Souza FJ. Performance of an optimized k− ϵ turbulence model for flowsaround bluff bodies. Mech Res Commun. 2020; 105: 103518.

37. Fontes DH, Duarte CAR, de Souza FJ. Numerical simulation of a water droplet splash: Effects of density interpolationschemes. Mech Res Commun. 2018; 90: 18-25.
38. Solnordal CB, Wong CY. Predicting surface profile evolution caused by solid particle erosion. Melbourne: Ninth International Conferenceon CFD in the Minerals and Process Industries; 2012. pp.10-12.
39. Roach PJ. Verification of codes and calculations. AIAA J. 1998; 36: 696-702.